Available online at www.sciencedirect.com
ScienceDirect
Biochimica et Biophysica Acta 1768 (2007) 21–29
Biochimica et Biophysica Acta BBA
www.elsevier.com/locate/bbamem

Expression and purification of two anti-CD19 single chain Fv fragments for targeting of liposomes to CD19-expressing cells

W.W.K. Cheng [a], D. Das [b], M. Suresh [b], T.M. Allen [a,*]

[a] 9-31 Medical Sciences Building, Dept. of Pharmacology, Faculty of Medicine and Dentistry, University of Alberta, Edmonton, Canada T6G 2H7
[b] Faculty of Pharmacy and Pharmaceutical Sciences, University of Alberta, Edmonton, Canada

Received 7 April 2006; received in revised form 22 August 2006; accepted 11 September 2006
Available online 19 September 2006

Abstract

Antibody-targeted liposomal anticancer drugs combine the specificity of antibodies with large payloads of entrapped drugs. We previously showed that liposomal doxorubicin (DXR) targeted via anti-CD19 monoclonal antibodies (mAb) or their Fab' fragments against the B-cell antigen CD19 led to improved therapeutic effects in murine B-cell lymphoma models relative to non-targeted liposomal DXR. We now are examining the use of anti-CD19 single chain fragments of the antibody variable region (scFv) as a targeting moiety, to test the hypothesis that scFv have advantages over full-sized mAb or Fab' fragments. We expressed two different anti-CD19 scFv constructs, HD37-C and HD37-CCH in *E. coli*, and purified the scFvs using two different methods. The HD37-CCH construct was selected for coupling studies due to its relative stability and activity in comparison to HD37-C. When coupled to liposomes, the HD37-CCH scFv showed increased binding in vitro to CD19-positive Raji cells, compared to non-targeted liposomes. Cytotoxicity data showed that HD37-CCH scFv-targeted liposomes loaded with DXR were more cytotoxic than non-targeted liposomal DXR. Our results suggest that anti-CD19 scFv constructs should be explored further for their potential in treating B-lymphoid leukemias and lymphomas.

Keywords: Anti-CD19; scFv; Liposome; Doxorubicin; B-lymphoid cell; Immunoliposome

1. Introduction

The use of antibodies and antibody fragments as cancer therapeutics have flourished in recent years and led to the clinical approval of several monoclonal antibodies, including Rituxan® (rituximab) and Herceptin® (trastuzumab) [1,2]. Currently, more than 150 mAbs are in clinical trials worldwide [3]. Immuno-conjugates, where mAbs are covalently linked to a few molecules of drugs, toxins or radioisotopes, have also been successfully commercialized, e.g., Zevalin® (ibritumomab tiuxetan), Bexxar (^{131}I-tositumomab), and Mylotarg® (gemtuzumab ozogamicin) [4–6]. Additive or synergistic effects have been demonstrated in patients when combinations of signaling antibodies such as rituximab and conventional chemotherapeutic drugs are administered [7,8].

Although mAbs can be highly selective for their targets, their properties are not ideal for continued administration in patients since immune reactions can occur, particularly to antibodies containing foreign (e.g., mouse) regions [9]. Antibody fragments, such as Fab' fragments (~55 kDa) and single chain fragments of the variable region (~35 kDa) lack the Fc antibody fragment, and thus the dominant immunogenic determinants. Fab' and scFv fragments can be selected by phage display and are more easily engineered than mAbs to control properties such as affinity or internalization capabilities [10]. They can be produced by a variety of methods including bacterial and algal fermentation, which should decrease their production costs [11]. Many laboratories are currently investigating the use of these small fragments for the treatment of cancers [12–17].

Liposomes are phospholipid bilayer spheres that can encapsulate drugs in their aqueous interior. The grafting of polyethylene glycol (PEG) to the surface of liposomes (termed Stealth® liposomes) serves two purposes: the polymer terminus is a convenient location for the coupling of targeting ligands such as mAbs and derived fragments, and these liposomes have circulation half-lives of several hours, which allows sufficient

* Corresponding author. Fax: +1 780 492 8078.
E-mail address: terry.allen@ualberta.ca (T.M. Allen).

0005-2736/$ - see front matter © 2006 Elsevier B.V. All rights reserved.
doi:10.1016/j.bbamem.2006.09.004

time for the liposomes to access and bind to the target cells [13,15,18,19]. Several liposomal drugs are currently on the market, including Caelyx/Doxil® (a Stealth® liposomal formulation of the anticancer drug doxorubicin (DXR), which is approved for AIDS-related Kaposi's sarcoma, refractory ovarian and metastatic breast cancers) [20]. Currently no ligand-targeted liposomes are in the clinic, but extensive preclinical research activity is taking place in this area. The concept is similar to that of antibody-drug conjugates, with the advantage that targeted liposomes can deliver a far greater payload of drug per antibody, i.e., several hundred drug molecules per antibody, relative to less than 10 drug molecules per antibody for the antibody–drug conjugates. This can result in increased therapeutic effect for fewer antibodies, leading to reduced antibody-associated side effects and reduced expense [20–23].

We have had a long-standing interest in disease targets that are readily accessible from the vasculature, including B and T cell haematological malignancies and the vasculature of solid tumors. Non-Hodgkin's lymphoma, the most common B-cell malignancy, is the 5th most common cause of new cases of cancer in North America and accounts for approximately 4 to 5% of new cases of cancer every year [24,25]. B-cell malignancies generally respond well to initial chemotherapy, especially the combination of Rituxan® plus CHOP (cyclophosamide, doxorubicin, vincristine and prednisone) [8,26,27]. Unfortunately, a substantial percentage of patients who respond to initial therapy will relapse. This is thought to result from the incomplete eradication of residual malignant B-lymphoid cells and/or their progenitors, and justifies the search for therapies that can eradicate these cells. The CD19, CD20 and CD22 antigens are expressed on a high percentage of malignant B-lymphoid cells in lymphoma patients [25,28,29]. Since these antigens are found primarily on mature B cells and not on their precursor cells, they are good targets for directing therapeutics against malignant B-lymphoid cells.

We had previously shown that anti-CD19-targeted liposomal DXR led to improved therapeutic effects in murine models of human B lymphoma (Namalwa) relative to free DXR or non-targeted liposomal DXR [16,18,30,31]. We are now exploring the potential advantages of using scFv fragments, in relation to mAb and Fab', for targeting liposomes to B-cell malignancies. In the current study, two constructs of anti-CD19 scFv were tested separately for ease of production from *E. coli* fermentation and for ease of purification, storage and stability. The most suitable candidate was selected and conjugated to liposomes. Cell binding and cytotoxicity of the anti-CD19 scFv immunoliposomes were compared to non-targeted liposomes.

2. Materials and methods

2.1. Materials

Hydrogenated soy phosphatidylcholine (HSPC) and methoxypoly(ethylene glycol) (MW 2000), covalently linked to distearoylphosphatidylethanolamine ($mPEG_{2000}$-DSPE), were generous gifts from ALZA Corporation, Inc. (Mountain View, CA). Cholesterol (Chol) and 1-oleoyl-2-[6-[(7-nitro-2-1,3-benzoxadiazol-4-yl)amino]hexanoyl]-*sn*-glycero-3-phosphoethanolamine (NBD-PE) were purchased from Avanti Polar Lipids (Alabaster, AL). Maleimide-derivatized PEG_{3400}-DSPE (Mal-PEG_{3400}-DSPE) was custom synthesized by Nektar Therapeutics (Huntsville, AL). Chol-[1,2-^{3}H-(*N*)] hexadecyl ether ([^{3}H]CHE, 1.48-2.22 TBq/mmol) and ^{125}I-NaI, 185 MBq were purchased from Perkin Elmer Life Sciences (Woodbridge, ON). Bio-Rad Protein Assay Reagent was purchased from Bio-Rad Laboratories (Mississauga, ON). β-mercaptoethanol (β-ME), 2-iminothiolane (Traut's Reagent), L-arginine (L-Arg), Protein L Agarose columns, goat anti-mouse fluorescein isothiocyanate (GAM-FITC) conjugate and RPMI 1640 media were obtained from Sigma Chemical Co. (St. Louis, MO). 1,4-dithiothreitol (DTT) was purchased from Fisher Scientific (Nepean, ON). Nuclepore polycarbonate membranes (pore sizes, 0.4, 0.2, 0.1, and 0.08 μm) were purchased from Northern Lipids (Vancouver, BC). Sephadex G-50, Sephadex G-25, Sepharose CL-4B and Aqueous Counting Scintillant (ACS) were purchased from Amersham Biosciences (Baie d'Urfe, PQ). Nickel-nitrilotriacetic acid (Ni-NTA) column and murine anti-polyhistidine (anti-His) mAb were purchased from Qiagen (Qiagen, Hilden, Germany). Penicillin-streptomycin-L-glutamine (P/S/G), and fetal bovine serum were obtained from Invitrogen (Burlington, ON). Bacto Tryptone, Bacto Yeast Extract and Bacto Agar were from BD (Sparks, MD). All other chemicals were of the highest grade possible.

2.2. Cell lines and antibodies

The human Burkitt's lymphoma cell lines (Namalwa and Raji) and the human T-lymphoma cell line (Molt 4) were purchased from the American Type Culture Collection. The cells were cultured in suspension in RPMI 1640 media supplemented with 10% (V/V) fetal bovine serum, and 1% (V/V) P/S/G in a humidified 37 °C incubator with a 5% CO_2 atmosphere. Cell surface expression of CD19 was determined using single-color flow cytometry. Briefly, 1×10^6 cells were stained with a CD19 mAb, followed by a secondary antibody, GAM-FITC. Cell-associated fluorescence was analyzed on a Becton Dickinson FACScan using Lysis II software (Becton Dickinson, San Jose, CA).

The murine anti-CD19 mAbs, FMC63 mAb (IgG_{2a}) and HD37 mAb (IgG_1), were produced from the FMC63 [32] and HD37 hybridomas [33], obtained from Dr. H. Zola (Children's Health Research Institute, Adelaide, Australia) and Dr. B. Doerken (Charité, University Medicine, Berlin, Germany) via Dr. E. Vitetta (University of Texas Southwestern Medical Center, Dallas, TX), respectively. Two scFv constructs were used. The scFvs from the HD37 mAb were courtesy of Dr. S. Kipriyanov from Affimed Therapeutics AG, Heidelberg, Germany [34]. HD37-c-*myc*-Cys-His5 scFv (HD37-CCH) contains the c-*myc* and His5 tags for identification and purification, and a cysteine residue for coupling to liposomes. HD37-Cys (HD37-C) scFv, which contains a terminal cysteinyl residue for coupling to liposomes, was prepared by removing the tags from a HD37-c-*myc*-His6-Cys (HD37-CHC) construct as described below.

The PCR method was used to amplify the HD37-C scFv from HD37-c-*myc*-His6-Cys (HD37-CHC) in the pSKK vector [35]. Gene specific primers (forward primer, P1, 5' CTG CTG GCA GCT CAG CCG GCC ATG GCG CAG 3'; and Backward primer, P2, 5' TTA GCA CAG GCC TCT AGA TTA GCA GGA TCC AGC ATC AGC CCG TTT GAT TTC CAG CTT GGT GCC 3') were designed with suitable restriction enzyme sites (*Nco*I in P1 and *Xba*I in P2) in both primers, respectively, and a Cys codon was added before the stop codon in the P2 primer. PCR products were analysed by 1% agarose/TAE (40 mM Tris, 20 mM acetic acid, 1 mM EDTA) gel electrophoresis and amplified products were purified using a QIAquick gel extraction kit (Qiagen, Germany). Both the PCR product and the pSKK vector were digested with *Nco*I+*Xba*I endonucleases, gel purified and ligated overnight at 14 °C. The ligation mixture was transformed into *E. coli* Top10F electrocompetent cells (Invitrogen, Burlington, ON) by electroporation. Recombinant clones were screened by restriction digestion fragment analysis of the plasmid DNA, digested with *Nco*I and *Xba*I endonucleases. Digested products were analyzed by 1% agarose/TAE gel electrophoresis and the correct size insert was confirmed by restriction digestion fragment mapping.

2.3. Expression of scFv clones

For HD37-C, a recombinant plasmid carrying the scFv gene was used to transform *E. coli* RV308 by a heat shock method [36]. *E. coli* RV308 transformants were propagated in 5 mL of 2YT (1.6% tryptone, 1% yeast extract and 0.5% NaCl, pH 7.5), containing 100 μg/mL of ampicillin, and were

incubated at 26 °C with shaking at 250 rpm until an optical density at 600 nm (OD_{600}) of approximately 0.8 was reached. The bacterial culture was induced with 1 mM isopropyl-beta-D-thiogalactopyranoside (IPTG) and allowed to grow for 16 h at 22 °C. Bacteria were then harvested by centrifugation at 5000×*g* for 10 min at 4 °C and a total cell lysate was prepared by addition of sample buffer to the pellet and heating at 95 °C for 5 min [36]. Total cell protein was analyzed by SDS-PAGE using 10% polyacrylamide gels performed according to Laemmli [37] with a Mini Protean II apparatus (Bio-Rad). The protein gel was stained with 0.25% Coomassie Brilliant Blue R-250.

2.4. Western blot analysis of expressed scFv constructs

Total cell protein was separated on SDS-PAGE using a 10% Tris SDS-PAGE gel and transferred to a Hybond ECL nitrocellulose membrane [38] using a Trans-Blot apparatus (Bio-Rad, Mississauga, ON) following manufacturer's instructions. The ECL membrane was blocked with 5% skim milk in 0.1% Tween 20 in phosphate buffer saline, pH 7.3 (PBST) for 1 h. The membrane was washed with PBST and incubated with Protein-L horse-radish peroxidase (HRP) and anti-His mAb for 1 h. After incubation, the membrane was washed with PBST and incubated with goat anti-mouse HRP (GAM-HRP, Upstate, Lake Placid, NY). In some cases the membranes were reacted with Protein-L-HRP for 1 h. Finally, the membrane was washed 4 times with PBST and enhanced chemiluminescent-based detection was done according to the manufacturer's protocol (ECL Western blot analysis system, Amersham Biosciences, PQ).

2.5. Expression and extraction of HD37-C and HD37-CCH from the periplasmic space and inclusion bodies

The scFv constructs were expressed using the pSKK vector in RV 308 *E. coli* in shaker cultures as described above. Expression of the scFvs was induced with 0.2 mM of IPTG at 22 °C when OD_{600} reached 0.8. Cells were harvested by centrifugation after 16 h of induction.

For extraction of HD37-C from the periplasmic space of *E. coli*, cells were incubated with the periplasmic extraction buffer (100 mM Tris HCl, 20% W/V sucrose, 1 mM EDTA, pH 8.0) for 1 h on ice. Cells were then centrifuged and the extracted scFv fragments were collected in the supernatant as periplasmic extract. The HD37-C scFv was purified from the periplasmic extract using a Protein L agarose column as previously described [35]. Briefly, the periplasmic extract was extensively dialyzed in phosphate buffered saline (PBS) at pH 7.4 before loading onto the column at 20 mL/h, using a peristaltic pump. The column was washed with PBS (pH 7.4) to remove non-specifically bound proteins. The scFv was eluted with elution buffer (100 mM glycine, pH 2.0) and immediately neutralized with addition of 1 M Tris at pH 9.0 to achieve a final pH of 7.4. Fractions were analyzed by SDS-PAGE and Western blot.

Alternatively, HD37-C was isolated from inclusion bodies and was purified as previously described with slight modification [35]. Cell pellets from periplasmic extraction were resuspended in Lysis Buffer 1 (50 mM Tris, 200 mM NaCl, 1 mM EDTA, pH 8.0) and lysed by either French Press or sonication. The cells were then centrifuged at 10,000×*g* at 4 °C and the inclusion bodies were collected as pellets. The inclusion bodies were resuspended and incubated in 0.1% Triton X-100 for 0.5 h at room temperature and were then centrifuged at 10,000×*g* at 4 °C. The inclusion bodies were washed with Lysis Buffer 1 and resuspended in Lysis Buffer 2 (100 mM Tris, 200 mM NaCl, 1 mM EDTA, pH 8.3). A previously described step-wise dialysis method, with modification, was used for refolding the denatured HD37-C [39]. Inclusion bodies were solubilized in Lysis Buffer 2 containing 6 M guanidine hydrochloride (Gu HCl) and centrifuged at 10,000×*g* at 4 °C. Soluble protein was collected in the supernatant and before dialysis the protein concentration was adjusted to 100 μg/mL. Dialysis was conducted with sequential daily decreases of Gu HCl (6, 3, 2, 1, 0.5, 0 M). At the 1 M and 0.5 M Gu HCl stages, 400 mM of L-arginine and 375 μM of oxidized glutathione (GSSG) were added to assist the proper formation of disulfide bonds.

The procedure for extracting HD37-CCH from the periplasmic space was the same as for HD37-C. After extraction, the periplasmic extract, containing the HD37-CCH scFv, was extensively dialyzed in NI-NTA Dialysis Buffer (1 M NaCl, 50 mM Tris HCl and 40 mM imidazole, pH 7.0). The dialyzed extract was then incubated overnight at 4 °C with Ni-NTA at a 50:1 (V:V) ratio, with gentle rocking. After the incubation, the Ni-NTA was packed into a column and washed with washing buffers (1 M NaCl, 50 mM Tris HCl, and 50 or 80 mM imidazole, pH 7.0). The HD37-CCH was then eluted with elution buffer (1 M NaCl, 50 mM Tris HCl and 300 mM imidazole, pH 7.0). Elution fractions were analyzed on SDS-PAGE gels and scFv-containing fractions were extensively dialyzed in PBS.

2.6. Preparation of liposomes

Non-targeted Stealth® liposomes (SL) were composed of HSPC:CHOL:$mPEG_{2000}$-DSPE at a 2:1:0.10 phospholipid molar ratios. Stealth® immunoliposomes (SIL) were composed of HSPC:CHOL:$mPEG_{2000}$-DSPE:Mal-PEG_{3400}-DSPE at a molar ratio to HSPC of 2:1:0.08:0.02. [^{3}H]CHE was added as a non-exchangeable, non-metabolized lipid tracer [40,41]. Liposomes were prepared as previously described [30]. Briefly, the lipid film was dried by rotovaporation for 1 h and then placed in a high vacuum overnight. The lipid films were hydrated at a concentration of 10–30 mM phospholipid (PL) with PBS (pH 8.0). Hydrated liposomes were extruded at 65 °C through a series of Nuclepore polycarbonate filters, with pore sizes from 0.4 μm to 0.08 μm, resulting in an average final diameter in the range of 100±20 nm. The sizes of liposomes were determined using dynamic light scattering (Brookhaven BI-90 Particle Sizer, Holtsville, NY).

2.7. Preparation of immunoliposomes

HD37-C and HD37-CCH scFv fragments were coupled to liposomes containing Mal-PEG-DSPE at a 1:500 scFv:HSPC molar ratio, as previously described, with slight modifications [42]. The scFv fragments were reduced for 1 h at room temperature with 14 mM β-ME and with 5 mM DTT for HD37-C and HD37-CCH, respectively. ^{125}I-labeled scFvs were used as tracers. Unreacted reducing agents were removed from samples by Sephadex G-25 columns. ScFv fragments were quickly combined with liposomes containing Mal-PEG_{3400}-DSPE and were allowed to incubate overnight at room temperature with stirring.

HD37 and FMC63 mAbs were thiolated with Traut's reagent at a ratio of Traut's:IgG of 20:1 (mol/mol) in degassed HBS (pH 8.0) for 1 h. After thiolation, unreacted Traut's reagent was removed from the sample via Sephadex G-50 columns equilibrated with degassed HBS (pH 7.4). ^{125}I-labeled HD37 and FMC63 mAbs were used as tracers. Immediately after the column, the thiolated antibody was added to liposomes at 1:1000 mAb:HSPC molar ratio and incubated overnight at room temperature with stirring. Unconjugated antibody and antibody-free liposomes were removed by chromatography on Sepharose CL-4B columns in PBS, pH 8.0.

2.8. Flow cytometry studies

Fluorescence-activated cell sorting (FACS) experiments were conducted to determine the binding of HD37-CCH scFvs to Raji cells. Briefly, 1×10^6 cells in the exponential growth phase were seeded in sterile tubes. Cells were incubated with scFvs for 1 h at 4 °C, and then washed with cold PBS. Binding of scFvs was detected in a Becton Dickinson FACScan (BD Biosciences, Mississauga, ON) after labeling with murine anti-His mAb followed by GAM-FITC. The binding of scFvs to Raji cells was indicated by rightward shifts in the fluorescence peak.

Experiments to determine equilibrium dissociation constants (K_D) were performed as described with slight modifications [43]. Briefly, 2×10^5 Raji cells were incubated with various concentrations of HD37 mAb or HD37-CCH in PBS supplemented with 10% FBS (PBS/FBS) at a final volume of 1 mL for 3 h at 4 °C. Cells were then washed twice with PBS/FBS. For HD37-CCH, cells were then incubated with 20 μL of murine anti-His mAb (200 ng/mL) in PBS/FBS for 1 h at 4 °C and then washed twice with PBS/FBS. Cells were then incubated with 20 μL of a 1/50 dilution of GAM-FITC in PBS/FBS for 30 min at 4 °C. Cells were washed twice with PBS/FBS and resuspended in 0.5 mL of 4% formaldehyde in PBS. Fluorescence was measured in a Becton Dickinson FACScan and were normalized using the SPHERO™ FITC Calibration Particle Kit (Spherotech, Libertyville, IL).

2.9. In vitro cellular binding studies using tritium-labeled liposomes

Cellular binding studies were performed as previously described [31]. The association with B-lymphoid cells was determined for targeted and non-targeted

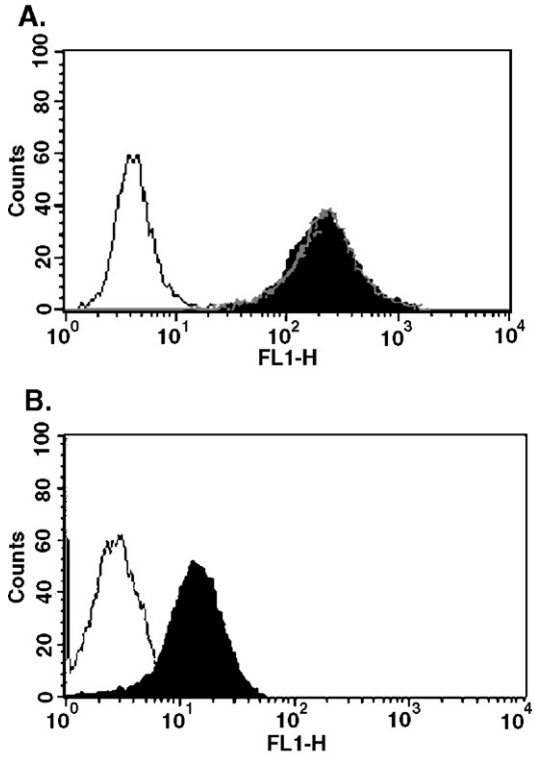

Fig. 1. Flow cytometry analysis. (A) 1×10^6 Namalwa cells treated with 10 μg of either FMC63 mAb or HD37 mAb. Black: Control (no treatment), Grey: FMC63 mAb, Black Solid: HD37 mAb. (B) Binding of periplasmic extracted HD37-CCH with Raji cells. Black: control (no treatment); Black, solid: HD37-CCH. Fluorescence shift to the right indicates binding to cells.

liposomes, labeled with [^{3}H]CHE. Briefly, 1×10^6 Raji or Namalwa cells were seeded in sterile tubes. Cells were incubated with various formulations of liposomes (SL, SIL[HD37-C], SIL[HD37-CCH], SIL[HD37 mAb] and SIL [FMC63 mAb]) for 1 h at 37 °C, at PL concentrations ranging from 0.1 to 3.2 mM. Cells were then washed 3 times with cold PBS, and the amount of [^{3}H] CHE counts associated with cells was determined by scintillation counting (Beckman LS-6800 Scintillation Counter, Beckman Coulter Canada, Inc., Mississauga, ON). Data were presented as nmol PL associated with 1×10^6 cells. Specific binding was calculated by subtracting cell-associated radioactivity counts of SL from SIL.

2.10. In vitro cytotoxicity studies

Cytotoxicity studies employed the MTT tetrazolium assay as previously described [18]. Briefly, 8×10^5 Raji cells or 5×10^5 Molt 4 cells were incubated with DXR-loaded SIL[HD37-CCH] (SIL-DXR[HD37-CCH]); SL-DXR; a mixture of unconjugated HD37-CCH and SL-DXR (HD37-CCH+SL-DXR); free HD37-CCH or free DXR for 1 h at 37 °C. Cells were then thoroughly washed and were allowed to grow for another 48 h in full media. Treated cells were compared to untreated cells to calculate percent of viable cells. In these experiments, the commercially available liposomal DXR, Caelyx®, was used as the non-targeted SL-DXR.

3. Results

Using FACS, we demonstrated that both parental full-length CD19 mAbs, FMC63 and HD37, bound to the B-lymphoid cell lines Namalwa and Raji (Fig. 1A). As well, the scFv fragment, HD37-CCH, extracted from the periplasmic space also bound to Raji cells (Fig 1B). Using a Lineweaver–Burk analysis, the K_D of FMC63 mAb was found to be 1.1×10^{-9} M (not shown). The K_D of the HD37 whole mAb was 2.7×10^{-9} M, which was approximately 3-fold lower than that of the scFv fragment, HD37-CCH (8.1×10^{-9} M) (not shown).

Since the presence of the His6 and c-*myc* tags might interfere with the eventual clinical applications of scFv fragments, we removed the His6 and c-*myc* tags from the HD37-CHC construct, forming HD37-C (Fig. 2). The HD37-C protein had a molecular mass of approximately 29 kDa as evident from SDS-PAGE (Fig. 2A). Western blot analysis suggested the presence of the variable regions in our target protein (Fig. 2B). In addition, the His6 tag was not detected in the scFv (Fig. 2C). A positive control, HD37-CHC, containing the His6 tag, showed that the anti-His mAb was functioning properly.

In order to further investigate the binding activity of the refolded HD37-C, we coupled the scFv, trace-labeled with ^{125}I,

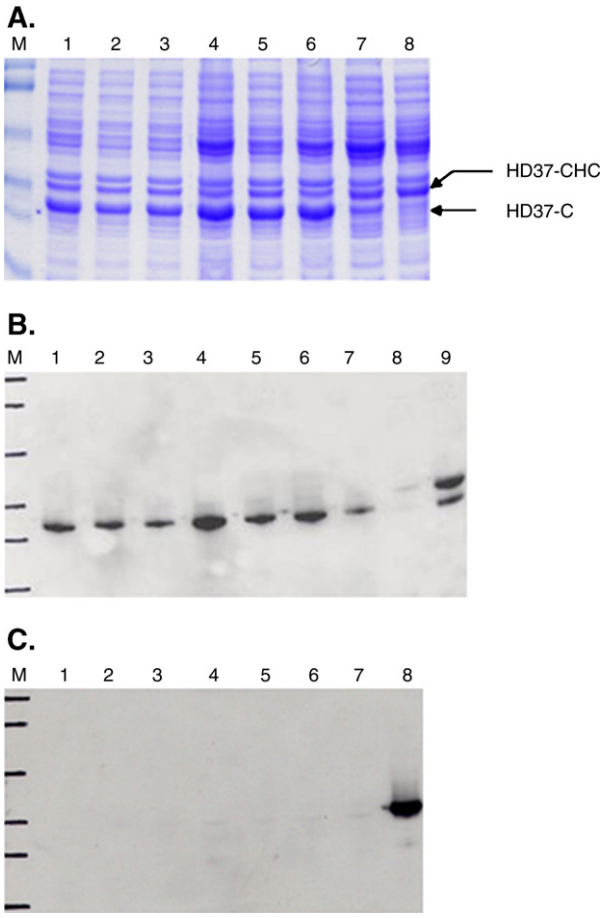

Fig. 2. SDS-PAGE and Western blot Analysis of HD37-C scFv fragments. (A) SDS-PAGE gel of total cell lysates of bacteria expressing HD37-C. (C) Western blot of total cell lysates probed with murine anti-His mAb and then GAM-HRP (A and C) Lane M, molecular weight marker; Lanes 1–6, representative samples of induced RV308 clones expressing HD37-C; Lane 7, HD37-C-expressing RV308 clone without induction; Lane 8, positive control (HD37-CHC containing cell lysate). (B) Western blot of total cell lysates probed with Protein L-HRP. Lane M, molecular weight marker; Lanes 1–6 representative samples of induced RV308 clones expressing HD37-C; Lane 7, HD37-C-expressing RV308 clone without induction; Lanes 8 and 9, positive control (HD37-CHC containing cell lysate) loaded at low and high concentrations, respectively.

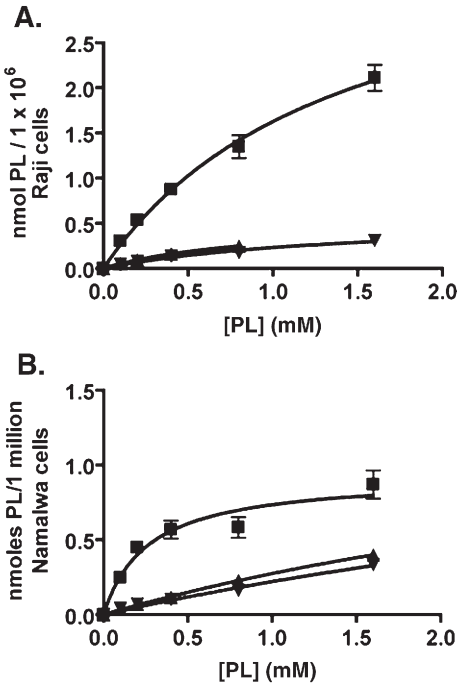

Fig. 3. Binding of immunoliposomes to B-lymphoid cells. 1×10^6 Raji cells were incubated with the various liposome formulations at increasing PL concentrations. (A) Raji cells. ■ SIL[HD37 mAb], ▲ SIL[HD37-C] and ▼ SL. (B) Namalwa cells. ■ SIL[FMC63 mAb], ▲ SIL[HD37-C] and ▼ SL.

to the surface of liposomes that were labeled with ^{3}H-CHE. Coupling densities of 19.2–25.6 μg scFv/μmol PL were obtained (30–40% coupling efficiency), which compares favourably with previous literature values [17]. The binding to B-lymphoid cells in vitro was compared for SIL[HD37-C], non-targeted liposomes (SL), and either SIL[HD37 mAb] or SIL[FMC63 mAb] (Fig. 3A, B). SIL[HD37-C] had low binding to CD19-positive Raji or Namalwa cells, which was not different from control SL and was substantially lower than the binding of liposomes targeted via the FMC63 or HD37 mAbs.

When the HD37-CCH construct was purified from periplasmic extracts, modest yields of 0.4–0.6 mg/L culture were obtained. The scFv was present in whole cell lysates and periplasmic extracts (Fig. 4B) and was enriched in eluate fractions after affinity purification (Fig. 4A, B). The purified protein bound to CD19-positive cells (Fig. 1B) and was stable in PBS. The purified HD37-CCH scFv was coupled to liposomes at a coupling density of 14–20 μg/μmol PL (20–29% coupling efficiency). SIL[HD37-CCH] showed increased binding to Raji cells compared to SL (Fig. 5A, B) and the increased binding was abolished when cells were pre-incubated with the whole HD37 mAb in a competition experiment. Thus, binding of SIL[HD37-CCH] was specific to CD19. In another control, a mixture of unconjugated HD37-CCH and SL did not result in an increase in binding compared to SL. Specific binding of SIL[HD37-CCH] at 37 °C (permissive for internalization) and 4 °C (non-permissive for internalization) were also compared (Fig. 5C). Increased liposome uptake occurred at 37 °C relative to 4 °C, probably due to recycling of CD19 at 37 °C following receptor-mediated internalization. When binding of SIL[HD37-CCH] to CD19-negative Molt 4 control cells was tested, there was no difference between the binding of SIL[HD37-CCH] and SL (Fig. 5D). We also compared the binding of SIL[HD37-CCH] and SIL[HD37 mAb] to Raji cells. Taking into consideration that each mAb has two antigen binding sites, the number of available binding sites on SIL[HD37-CCH] and SIL[HD37 mAb] were 0.45 nmol/μmol PL (16 μg scFv /μmol PL) and 0.32 nmol/μmol PL (25 μg mAb /μmol PL) respectively. At similar numbers of available binding sites on the surfaces of liposomes, the uptake of SIL[HD37 mAb] at 37 °C was significantly better than for the SIL[HD37-CCH] (Fig. 5E).

In vitro MTT cytotoxicity study, with a 1 h incubation, demonstrated that SIL-DXR[HD37-CCH] were approximately 11-fold more cytotoxic to Raji cells than untargeted SL-DXR. The concentrations of drugs inhibiting 50% of cell growth (IC_{50}'s) were 21±9 μM, 244±36 μM and 225±33 μM for SIL-DXR[HD37-CCH], SL-DXR and HD37-CCH+SL-DXR, respectively. The IC_{50} for the free drug was 0.7±4 μM. There was no toxicity observed when Raji cells were treated with free HD37-CCH at concentrations which were typically found on the surface of SIL-DXR[HD37-CCH]. IC_{50}'s for Molt 4 cells

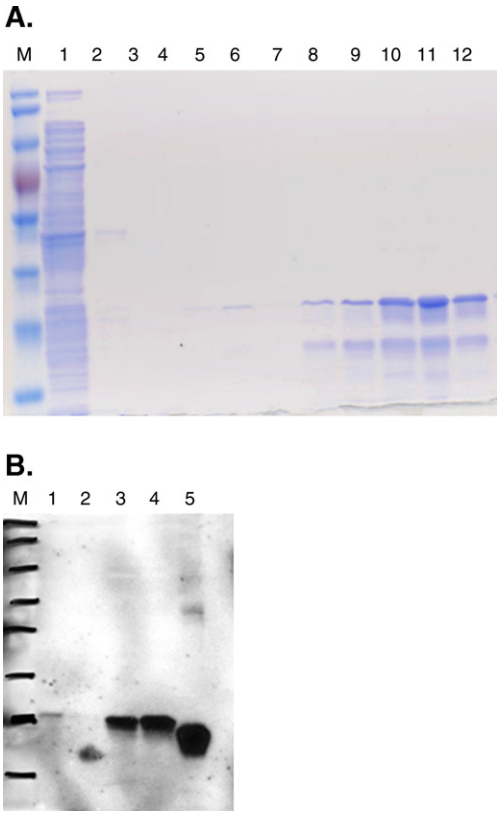

Fig. 4. Purification of HD37-CCH after periplasmic extraction. (A) SDS-PAGE gel of purified HD37-CCH after purification using a Ni-NTA column. Lane M, molecular weight markers; Lane 1, unbound fraction; Lanes 2–7, wash fractions; lanes 8–12, eluted fractions of scFv. (B) Western blot of HD37-CCH fragments, detected using murine anti-His mAb and then GAM-HRP. Lane M; molecular weight markers: Lanes 1 and 2: periplasmic extracts; Lanes 3 and 4: purified HD37-CCH; Lane 5: positive control (poly-His-containing scFv).

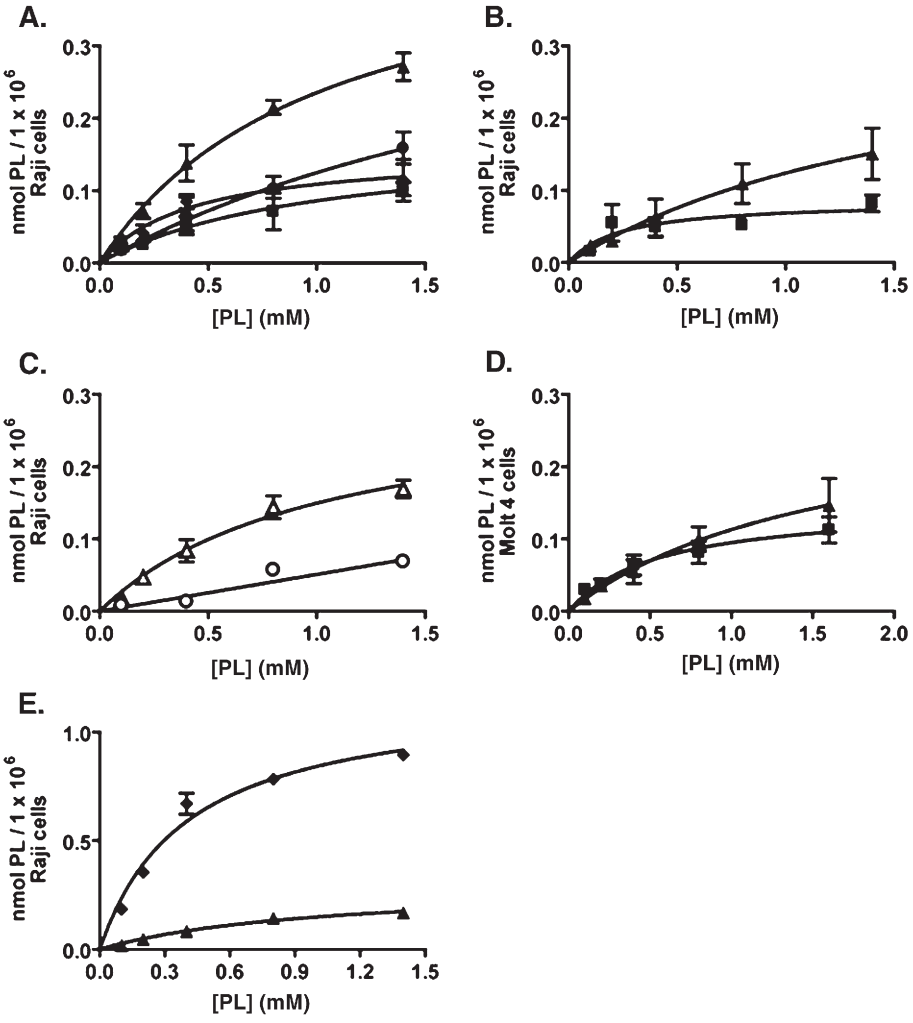

Fig. 5. Binding of SIL[HD37-CCH] to Raji cells. 1×10^6 Raji cells were incubated with increasing PL concentrations of SIL[HD37-CCH] or SL for 1 h. For the competition study, Raji cells were pre-incubated with 100 μg of HD37 mAb (7.5- to 120-fold excess) for 15 min. Binding was measured by scintillation counting of the liposomal ^{3}H-CHE label. (A) Binding at 37 °C. ▲ SIL[HD37-CCH], ● SIL[HD37-CCH]+HD37 mAb, ♦ HD37-CCH+SL, ■ SL. (B) Binding at 4 °C. ▲ SIL[HD37-CCH], ■ SL. (C) Specific binding of SIL[HD37-CCH] at 37 and 4 °C. △ 37 °C, ○ 4 °C. (D) Binding to Molt 4 cells at 37 °C. ▲ SIL[HD37-CCH], ■ SL. (E) Specific binding of SIL[HD37-CCH] and SIL[HD37 mAb] at 37 °C. ▲ SIL[HD37-CCH], ♦ SIL[HD37 mAb].

treated with SIL-DXR[HD37-CCH], SL-DXR and free DXR to be 136±42 μM , 106±20 μM, and 0.3±0.1 μM respectively.

4. Discussion

FMC63 and HD37 effectively bound to the B-lymphoid cell lines, and both mAbs produced a greater than 2 log shift in fluorescence, indicating efficient binding of the mAbs to the CD19 antigen on intact cells. Binding profiles to Raji cells of both antibodies were similar to those obtained with Namalwa cells (not shown). The HD37-CCH scFv, also interacted efficiently with Raji cells, producing approximately a 1 log shift in fluorescence intensity. Using the standard radiolabeled mAb assay, the reported equilibrium dissociation constant (K_D) for FMC63 mAb is 2.4×10^{-10} M, while the K_D of HD37 mAb is 3.3×10^{-9} M [44,45], which are similar to the results that we have determined.

In this study, a very low yield of native HD37-C scFv was obtained from the periplasmic space (~0.1 mg/L of culture), so we proceeded to isolate the scFv from inclusion bodies and obtained denatured scFv in much larger quantities (~1–2 mg/L culture). However, this scFv required refolding. We attempted to use a Protein L-FITC conjugate for detecting refolded HD37-C bound to CD19 using FACS, but no binding was observed. Therefore, we hypothesized that either the refolded HD37-C scFv had lost its activity due to improper refolding, or the Protein L-FITC conjugate was not able to bind to refolded HD37-C when the scFv was bound to CD19. To further investigate the activity of the refolded HD37-C, we conjugated the scFv to the surface of liposomes. The refolded HD37-C, when conjugated to liposomes, did not increase cell-binding of these liposomes to CD19-positive Raji cells, which suggest that the scFv fragments did not bind to CD19. Taken together, our results seem to support our hypothesis that the refolded HD37-C was not active.

The HD37-CCH scFv, when coupled to the surface of liposomes, resulted in specific and increase uptake of the immunoliposomes into Raji cells. The binding of SIL[HD37-

CCH] to Raji cells also resulted in internalization of these liposomes. These results are similar to published studies using the FMC63 mAb and Fab'-conjugated liposomes [16,18]. In these studies, the conjugation of the mAb and Fab' to the surfaces of liposomes led to internalization of the immunoliposomes, recycling of CD19 and higher binding/uptake at 37 °C than at 4 °C. We had observed a significant difference in cell-binding when SIL[HD37-CCH] was compared to SIL[HD37 mAb] at similar densities of binding sites on the surface of liposomes. We speculate that the decrease in uptake of SIL [HD37-CCH] is due to a decrease in affinity of the scFv for CD19 in comparison to the mAb. Normally, a decrease in affinity is observed when single chain fragments are compared to their parent mAb. This agrees with our observation of targeted liposomes where affinity of SIL[HD37-CCH] to Raji cells was decreased by approximately 3-fold when compared to SIL[HD37 mAb]. A decrease in avidity could also lead to the decreased binding of SIL[HD37-CCH]. Coupling ligands with single binding sites, e.g., Fab' or scFv, to liposomes will make them multivalent, but the degree to which this will restore avidity will depend on factors such as the ligand concentration and its degree of flexibility and orientation.

The increase in cytotoxicity of SIL-DXR[HD37-CCH] can be attributed to the targeting of the CD19 antigen and internalization of the liposome-drug package. For a 1 h incubation, prior to washing away the liposomes we would expect very little leakage of DXR from either the targeted or non-targeted formulation of liposomal DXR since they have leakage half lives in excess of 90 h [46]. Our cytotoxicity results with the HD37-CCH scFv fragment are consistent with our previous results, showing that DXR-loaded anti-CD19 mAb and Fab' immunoliposomes were more cytotoxic than SL. [16,19,30,47]. In addition, we have shown that the increase in cytotoxicity associated with SIL-DXR[HD37-CCH] is CD19-mediated. The IC_{50}'s of Raji cells, treated with a mixture of unconjugated SL-DXR+HD37-CCH and SL-DXR, and the IC_{50}'s of Molt 4 cells (CD19-negative) treated with either SIL-DXR[HD37-CCH] or SL-DXR, were similar.

In addition to the two constructs we have reported, we also experimented with another anti-CD19 scFv, the n-strep-His6-4G7-Gly4-Cys (nH-4G7-GC), kindly provided to us by Dr. G. Fey (Friedrich-Alexander University of Erlangen-Nuremberg, Germany). When extracted from the periplasm *E. coli*, the scFv bound effectively to CD19 (not shown). Because expression in the periplasmic space resulted in very low yields, the nH-4G7-GC was expressed in *E. coli* and extracted from inclusion bodies. However, unfolding and refolding of the scFv from inclusion bodies did not produce sufficient quantities of properly folded scFv for subsequent experimentation. During the refolding procedure following extraction from inclusion bodies, we postulate that the presence of a hydrophobic leader sequence in the scFv led to aggregation in the isotonic buffer, PBS.

Refolding of denatured scFv from inclusion bodies carries the potential of increased yield. This is especially important in the development of antibody or antibody fragments for clinical use, since large amounts of materials will be required. Although the refolding method can greatly increase production yield in comparison to periplasmic extraction of native proteins, it may not result in "usable" product. During the refolding process, the scFv can be trapped in a "thermodynamic sink", where the protein remains in an intermediate state [48]. This thermodynamic sink can lead to incomplete refolding, resulting in loss of activity and aggregation.

Antibody-targeted liposomal drugs can selectively deliver large payloads of drugs to cancer cells. Small antibody fragments, such as scFv, can reduce the immunogenicity associated with larger fragments of foreign origin. Many groups have demonstrated the potential of using scFvs as targeting moieties for liposomal anticancer drugs [14,17,49,50] and at least one formulation of scFv-coupled liposomal doxorubicin is near clinical testing [51]. In this study, we have employed two different methods for isolating scFv fragments from *E. coli*. We have found that, although isolating scFv from inclusion bodies with subsequent refolding can dramatically increase protein-yield, the purified scFv may not refold properly, leading to issues with activity and stability. On the other hand, extraction of the native scFv from the periplasmic space, although producing relatively smaller amounts of protein, resulted, in our hands, in proteins that are active and are relatively stable. Therefore, we have concluded that this is the method of choice for producing scFv fragments for our future studies. After some preliminary experiments with the HD37-C construct, we selected the HD37-CCH for our subsequent experiments due to its stability and affinity for the CD19 antigen. We have shown that, when the scFv is conjugated to the surface of liposomes, these HD37-CCH immunoliposomes can specifically bind to CD19-expressing cells and trigger internalization of the liposome package. Our initial cytotoxicity studies demonstrated that the doxorubicin-loaded SIL[HD37-CCH] was more cytotoxic than Caelyx®, a commercial formulation of non-targeted Stealth® liposomal doxorubicin. Future experiments will examine the in vivo pharmacokinetics properties and therapeutic activity of the SIL[HD37-CCH] in comparison to liposomes targeted with the HD37 mAb and HD37 Fab'.

Acknowledgements

We thank Dr. D.C. Drummond of Hermes Biosciences for insightful discussions on the purification of scFv fragments. We thank Dr. Heddy Zola of the Children's Health Research Institute for permission to use the FMC63 mAb. We thank Dr. Bernd Doerken of the Berlin Humboldt University for permission to use the HD37 mAb, obtained via Dr. Ellen Vitetta of the University of Texas Southwestern Medical Center and Dr. Georg Fey of the University of Erlangen-Nuremberg. We thank Dr. Sergei Kiprianov of Affimed Therapeutics for providing the HD37 scFv constructs, and for helpful discussions. Dr. Georg Fey provided much support and helpful discussions for this project. Funding for this project was provided by the Canadian Institute of Health Research (MOP-9127).

References

[1] P. McLaughlin, A.J. Grillo-Lopez, B.K. Link, R. Levy, M.S. Czuczman, M.E. Williams, M.R. Heyman, I. Bence-Bruckler, C.A. White, F. Cabanillas, V. Jain, A.D. Ho, J. Lister, K. Wey, D. Shen, B.K. Dallaire, Rituximab chimeric anti-CD20 monoclonal antibody therapy for relapsed indolent lymphoma: half of patients respond to a four-dose treatment program, J. Clin. Oncol. 16 (1998) 2825–2833.

[2] C.L. Vogel, M.A. Cobleigh, D. Tripathy, J.C. Gutheil, L.N. Harris, L. Fehrenbacher, D.J. Slamon, M. Murphy, W.F. Novotny, M. Burchmore, S. Shak, S.J. Stewart, M. Press, Efficacy and safety of trastuzumab as a single agent in first-line treatment of HER2-overexpressing metastatic breast cancer, J. Clin. Oncol. 20 (2002) 719–726.

[3] J.M. Reichert, C.J. Rosensweig, L.B. Faden, M.C. Dewitz, Monoclonal antibody successes in the clinic, Nat. Biotechnol. 23 (2005) 1073–1078.

[4] M.S. Kaminski, A.D. Zelenetz, O.W. Press, M. Saleh, J. Leonard, L. Fehrenbacher, T.A. Lister, R.J. Stagg, G.F. Tidmarsh, S. Kroll, R.L. Wahl, S.J. Knox, J.M. Vose, Pivotal study of iodine I131 tositumomab for chemotherapy-refractory low-grade or transformed low-grade B-cell non-Hodgkin's lymphomas, J. Clin. Oncol. 19 (2001) 3908–3911.

[5] E.L. Sievers, R.A. Larson, E.A. Stadtmauer, E. Estey, B. Lowenberg, H. Dombret, C. Karanes, M. Theobald, J.M. Bennett, M.L. Sherman, M.S. Berger, C.B. Eten, M.R. Loken, J.J. van Dongen, I.D. Bernstein, F.R. Appelbaum, M.S. Group, Efficacy and safety of gemtuzumab ozogamicin in patients with CD33-positive acute myeloid leukemia in first relapse, J. Clin. Oncol. 19 (2001) 3244–3254.

[6] T.E. Witzig, L.I. Gordon, F. Cabanillas, M.S. Czuczman, C. Emmanouilides, R. Joyce, B.L. Pohlman, N.L. Bartlett, G.A. Wiseman, N. Padre, A.J. Grillo-Lopez, P. Multani, C.A. White, Randomized controlled trial of yttrium-90-labeled ibritumomab tiuxetan radioimmunotherapy versus rituximab immunotherapy for patients with relapsed or refractory low-grade, follicular, or transformed B-cell non-Hodgkin's lymphoma, J. Clin. Oncol. 20 (2002) 2453–2463.

[7] J. Baselga, L. Norton, J. Albanell, Y.M. Kim, J. Mendelsohn, Recombinant humanized anti-HER2 antibody (Herceptin) enhances the antitumor activity of paclitaxel and doxorubicin against HER2/neu overexpressing human breast cancer xenografts, Cancer Res. 58 (1998) 2825–2831.

[8] B. Coiffier, E. Lepage, J. Briere, R. Herbrecht, H. Tilly, R. Bouabdallah, P. Morel, E. Van Den Neste, G. Salles, P. Gaulard, F. Reyes, C. Gisselbrecht, CHOP chemotherapy plus Rituximab compared with CHOP alone in elderly patients with diffuse large B-cell lymphoma, N. Engl. J. Med. 346 (2002) 235–242.

[9] G.G. Klee, Human anti-mouse antibodies, Arch. Pathol. Lab. Med. 124 (2000) 921–923.

[10] P. Holliger, P.J. Hudson, Engineered antibody fragments and the rise of single domains, Nat. Biotechnol. 23 (2005) 1126–1136.

[11] A.C. Roque, C.R. Lowe, M.A. Taipa, Antibodies and genetically engineered related molecules: production and purification, Biotechnol. Prog. 20 (2004) 639–654.

[12] J. Bhatia, S.K. Sharma, K.A. Chester, R.B. Pedley, R.W. Boden, D.A. Read, G.M. Boxer, N.P. Michael, R.H. Begent, Catalytic activity of an in vivo tumor targeted anti-CEA scFv:carboxypeptidase G2 fusion protein, Int. J. Cancer 85 (2000) 571–577.

[13] Y.S. Park, Tumor-directed targeting of liposomes, Biosci. Rep. 22 (2002) 267–281.

[14] C. Marty, B. Odermatt, H. Schott, D. Neri, K. Ballmer-Hofer, R. Klemenz, R.A. Schwendener, Cytotoxic targeting of F9 teratocarcinoma tumours with anti-ED-B fibronectin scFv antibody modified liposomes, Br. J. Cancer 87 (2002) 106–112.

[15] F. Pastorino, C. Brignole, D. Marimpietri, P. Sapra, E. Moase, T.M. Allen, M. Ponzoni, Doxorubicin-loaded Fab' fragments of anti-disialoganglioside immunoliposomes selectively inhibit the growth and dissemination of human neuroblastoma in nude mice, Cancer Res. 63 (2003) 86–92.

[16] P. Sapra, E.H. Moase, J. Ma, T.M. Allen, Improved therapeutic responses in a xenograft model of human B-lymphoma (Namalwa) for liposomal vincristine versus liposomal doxorubicin targeted via anti-CD19 IgG2a or Fab' fragments, Clin. Cancer Res. 10 (2004) 1100–1111.

[17] T. Volkel, P. Holig, T. Merdan, R. Muller, R.E. Kontermann, Targeting of immunoliposomes to endothelial cells using a single-chain Fv fragment directed against human endoglin (CD105), Biochim. Biophys. Acta 1663 (2004) 158–166.

[18] D.E. Lopes de Menezes, L.M. Pilarski, T.M. Allen, In vitro and in vivo targeting of immunoliposomal doxorubicin to human B-cell lymphoma, Cancer Res. 58 (1998) 3320–3330.

[19] P. Sapra, T.M. Allen, Improved outcome when B-cell lymphoma is treated with combinations of immunoliposomal anticancer drugs targeted to both the CD19 and CD20 epitopes, Clin. Cancer Res. 10 (2004) 2530–2537.

[20] H. Maeda, J. Wu, T. Sawa, Y. Matsumura, K. Hori, Tumor vascular permeability and the EPR effect in macromolecular therapeutics: a review, J. Controlled Release 65 (2000) 271–284.

[21] D.C. Drummond, K. Hong, J.W. Park, C.C. Benz, D.B. Kirpotin, Liposome targeting to tumors using vitamin and growth factor receptors, Vitam. Horm. 60 (2001) 285–332.

[22] P. Carter, Improving the efficacy of antibody-based cancer therapies, Nat. Rev., Cancer 1 (2001) 118–129.

[23] T.M. Allen, Ligand-targeted therapeutics in anticancer therapy, Nat. Rev., Cancer 2 (2002) 750–763.

[24] R.T. Greenlee, M.B. Hill-Harmon, T. Murray, M. Thun, Cancer statistics, 2001, CA Cancer J. Clin. 51 (2001) 15–36.

[25] National Cancer Institute of Canada, Toronto 2005.

[26] M. Vose, B.K. Link, M.L. Grossbard, M. Czuczman, A. Grillo-Lopez, P. Gilman, A. Lowe, L.A. Kunkel, R.I. Fisher, Phase II study of rituximab in combination with CHOP chemotherapy in patients with previously untreated, aggressive non-Hodgkin's lymphoma, J. Clin. Oncol. 19 (2001) 389–397.

[27] P. Feugier, A. Van Hoof, C. Sebban, P. Solal-Celigny, R. Bouabdallah, C. Ferme, B. Christian, E. Lepage, H. Tilly, F. Morschhauser, P. Gaulard, G. Salles, A. Bosly, C. Gisselbrecht, F. Reyes, B. Coiffier, Long-term results of the R-CHOP study in the treatment of elderly patients with diffuse large B-cell lymphoma: a study by the Groupe d'Etude des Lymphomes de l'Adulte, J. Clin. Oncol. 23 (2005) 4117–4126.

[28] H.T.C. Chan, D. Hughes, R.R. French, A.L. Tutt, C.A. Walshe, J.L. Teeling, M.J. Glennie, M.S. Cragg, CD20-induced lymphoma cell death is independent of both caspases and the redistribution into Triton X-100 insoluble membrane rafts, Cancer Res. 63 (2003) 5480–5489.

[29] R. Luque, J.A. Brieva, A. Moreno, A. Manzanal, L. Escribano, J. Villarrubia, J.L. Velasco, J. Lopez-Jimenez, C. Cervero, M.J. Otero, J. Martinez, C. Bellas, E. Roldan, Normal and clonal B lineage cells can be distinguished by their differential expression of B cell antigens and adhesion molecules in peripheral blood from multiple myeloma (MM) patients—diagnostic and clinical implications, Clin. Exp. Immunol. 112 (1998) 410–418.

[30] D.E. Lopes de Menezes, M.J. Kirchmeier, J.-F. Gagne, L.M. Pilarski, T.M. Allen, Cellular trafficking and cytotoxicity of anti-CD19-targeted liposomal doxorubicin in B lymphoma cells, J. Liposome Res. 9 (1999) 199–228.

[31] D.E. Lopes de Menezes, L.M. Pilarski, A.R. Belch, T.M. Allen, Selective targeting of immunoliposomal doxorubicin against human multiple myeloma in vitro and ex vivo, Biochim. Biophys. Acta 1466 (2000) 205–220.

[32] H. Zola, P.J. Macardle, T. Bradford, H. Weedon, H. Yasui, Y. Kurosawa, Preparation and characterization of a chimeric CD19 monoclonal antibody, Immunol. Cell Biol. 69 (1991) 411–422.

[33] A. Pezzutto, B. Dorken, P.S. Rabinovitch, J.A. Ledbetter, G. Moldenhauer, E.A. Clark, CD19 monoclonal antibody HD37 inhibits anti-immunoglobulin-induced B cell activation and proliferation, J. Immunol. 138 (1987) 2793–2799.

[34] F. Le Gall, S.M. Kipriyanov, G. Moldenhauer, M. Little, Di-, tri- and tetrameric single chain Fv antibody fragments against human CD19: effect of valency on cell binding, FEBS Lett. 453 (1999) 164–168.

[35] D. Das, T.M. Allen, M.R. Suresh, Comparative evaluation of two purification methods of anti-CD19-c-*myc*-His(6)-Cys scFv, Protein Expression Purif. 39 (2005) 199–208.

[36] J. Sambrook, E.F. Fritsch, T. Maniatis, Molecular Cloning: A Laboratory Manual, Cold Spring Harbor Laboratory Press, New York, 1989.

[37] U.K. Laemmli, Cleavage of structural proteins during the assembly of the head of bacteriophage T4, Nature 227 (1970) 680–685.

[38] H. Towbin, T. Staehelin, J. Gordon, Electrophoretic transfer of proteins from polyacrylamide gels to nitrocellulose sheets: procedure and some applications, Proc. Natl. Acad. Sci. U. S. A. 76 (1979) 4350–4354.
[39] M. Umetsu, K. Tsumoto, M. Hara, K. Ashish, S. Goda, T. Adschiri, I. Kumagai, How additives influence the refolding of immunoglobulin-folded proteins in a stepwise dialysis system. Spectroscopic evidence for highly efficient refolding of a single-chain Fv fragment, J. Biol. Chem. 278 (2003) 8979–8987.
[40] G.L. Pool, M.E. French, R.A. Edwards, L. Huang, R.H. Lumb, Use of radiolabelled hexadecyl cholesterol ether as a liposome marker, Lipids 17 (1982) 445–452.
[41] J.T. Derksen, H.W. Morselt, G.L. Scherphof, Processing of different liposomal markers after in vitro uptake of immunoglobulin-coated liposomes by rat liver macrophages, Biochim. Biophys. Acta 931 (1987) 33–40.
[42] D. Kirpotin, J.W. Park, K. Hong, S. Zalipsky, W.-L. Li, P. Carter, C.C. Benz, D. Papahadjopoulos, Sterically stabilized anti-HER2 immunoliposomes: design and targeting to human breast cancer cells in vitro, Biochemistry 36 (1997) 66–75.
[43] C.A. Benedict, A.J. MacKrell, W.F. Anderson, Determination of the binding affinity of an anti-CD34 single-chain antibody using a novel, flow cytometry based assay, J. Immunol. Methods 201 (1997) 223–231.
[44] O.W. Press, A.G. Farr, K.I. Borroz, S.K. Andersen, P.J. Martin, Endocytosis and degradation of monoclonal antibodies targeting human B-cell malignancies, Cancer Res. 49 (1989) 4906–4912.
[45] I.C. Nicholson, K.A. Lenton, D.J. Little, T. DeCorso, F.T. Lee, A.M. Scott, H. Zola, A.W. Hohmann, Construction and characterisation of a functional CD19 specific single chain Fv fragment for immunotherapy of B lineage leukemia and lymphoma, Mol. Immunol. 34 (1998) 1157–1165.
[46] G.J.R. Charrois, T.M. Allen, Drug release rate influences the pharmacokinetics, biodistribution, therapeutic activity, and toxicity of pegylated liposomal doxorubicin formulations in murine breast cancer. Biochim. Biophys. Acta 1663 (2004) 167–177.
[47] P. Sapra, T.M. Allen, Internalizing antibodies are necessary for improved therapeutic efficacy of antibody-targeted liposomal drugs, Cancer Res. 62 (2002) 7190–7194.
[48] M. Hoyer, K. Ramm, A. Pluckthun, A kinetic trap is an intrinsic feature in the folding pathway of single-chain Fv fragments, Biophys. Chem. 96 (2002) 273–284.
[49] C. Mamot, D.C. Drummond, U. Greiser, K. Hong, D.B. Kirpotin, J.D. Marks, J.W. Park, Epidermal growth factor receptor (EGFR)-targeted immunoliposomes mediate specific and efficient drug delivery to EGFR- and EGFRvIII-overexpressing tumor cells, Cancer Res. 63 (2003) 3154–3161.
[50] C. Marty, Z. Langer-Machova, S. Sigrist, H. Schott, R.A. Schwendener, K. Ballmer-Hofer, Isolation and characterization of a scFv antibody specific for tumor endothelial marker 1 (TEM1), a new reagent for targeted tumor therapy, Cancer Lett. 235 (2006) 298–308.
[51] D.F. Nellis, D.L. Ekstrom, D.B. Kirpotin, J. Zhu, R. Andersson, T.L. Broadt, T.F. Ouellette, S.C. Perkins, J.M. Roach, D.C. Drummond, K. Hong, J.D. Marks, J.W. Park, S.L. Giardina, Preclinical manufacture of an anti-HER2 scFv-PEG-DSPE, liposome-inserting conjugate. 1. Gram-scale production and purification, Biotechnol. Prog. 21 (2005) 205–220.